Biomatter 4, e28534; March 2014; © 2014 Landes Bioscience

Alternative technique for calcium phosphate coating on titanium alloy implants

Van Quang Le[1], Geneviève Pourroy[1], Andrea Cochis[2], Lia Rimondini[2,3], Wafa I Abdel-Fattah[4], Hadeer I Mohammed[5], and Adele Carradò[1,*]

[1]Institut de Physique et Chimie des Matériaux de Strasbourg CNRS-UMR 7504; Strasbourg, France; [2]Department of Health Sciences; Università del Piemonte Orientale "Amedeo Avogadro"; Novara, Italy; [3]Consorzio Interuniversitario Nazionale per la Scienza e Tecnologia dei Materiali; Firenze, Italy; [4]Biomaterials Department; National Research Centre; Cairo, Egypt; [5]Biophysics Department; Ain Shams University; Cairo, Egypt

Keywords: hydroxyapatite, titanium alloy, chemical route, calcium-phosphate, physico-chemical characterization

As an alternative technique for calcium phosphate coating on titanium alloys, we propose to functionalize the metal surface with anionic bath containing chlorides of palladium or silver as activators. This new deposition route has several advantages such as controlled conditions, applicability to complex shapes, no adverse effect of heating, and cost effectiveness. A mixture of hydroxyapatite and calcium phosphate hydrate is deposited on the surface of Ti-6Al-4V. Calcium phosphate coating is built faster compared with the one by Simulated Body Fluid. Cell morphology and density are comparable to the control one; and the results prove no toxic compound is released into the medium during the previous seven days of immersion. Moreover, the cell viability is comparable with cells cultivated with the virgin medium. These experimental treatments allowed producing cytocompatible materials potentially applicable to manufacture implantable devices for orthopedic and oral surgeries.

Introduction

Metallic artificial implants are widely used as medical devices to replace, support or enhance an existing biological structure. Most of the orthopedic or dental implants are made of titanium alloys due to their advanced mechanical properties and excellent biocompatibility.[1] Per-Ingvar Brånemark[2] first discovered the principles of osteointegration in the 1950s. Pure titanium (Ti) was placed in a rabbit fibula, connected directly to the bone and did not induce any severe inflammatory or other reactions in skin or bone tissues. This unique property of titanium, allowing direct contact and connection to be developed between living bone and metal surface without soft tissue interface, has now multiple applications such as dental implants, craniofacial prosthesis, hip replacements, etc.

Besides titanium itself, Ti-6Al-4V is one of the most commonly used materials for medical implants because of its suitable mechanical properties, its corrosion resistance and relative inertia toward living tissues. Despite that, there are some uncertainties concerning the release of Al and V ions under certain conditions.[3] Nevertheless, the essential requirements for any artificial implanted material, especially metallic ones, are demonstrated to possess not only biocompatibility, but also bioactivity with the host. Indeed, several months are required to get a sufficient osteointegration, and in numerous cases, the osteointegration is incomplete. Thus, considerable work has been done to investigate various surface modification methods to increase the osteointegration rate such as surface-roughening (e.g., sandblasting and/or acid etching) and coating with hydroxyapatite (HA) $Ca_{10}(PO_4)_6(OH)_2$. Several physical and chemical methods were reported in the literature to modify titanium implants surfaces such as the plasma spray, magnetron sputtering, dip- and spin-coating sol-gel suspensions, soaking, electrophoresis, pulsed laser deposition, and biomimetic routes.

Since the 1960s, calcium phosphates (Ca-P) and mainly hydroxyapatite (HA) have been widely used in bone surgeries as they easily bond with bone once they are implanted, in spite of their poor mechanical characteristics.[4] The elaboration of bioactive ceramic coatings on metallic and non-metallic substrates implanted into the human body is, therefore, a way to combine the mechanical properties of the substrate and the bioactivity of the ceramic layer. To achieve fast and long-term bioactive surfaces, implant surfaces should be coated with a developed Ca-P for its superior biocompatibility and bioactive acting as a barrier against ion release.[5]

In the late 80s, the development of osteoconductive HA plasma spray coatings[6] on metallic prostheses allowed to improve the biological behavior of the metallic surface. Although plasma spray technique is currently employed to produce clinically-used coatings, the long-term stability of the coating/implant is questionable. The poor coating, substrate adherence and the lack of uniformity of the coating affect the implant long-term lifetime.

*Correspondence to: Adele Carradò; Email: carrado@unistra.fr
Submitted: 01/09/2014; Revised: 03/10/2014; Accepted: 03/14/2014; Published Online: 03/19/2014
http://dx.doi.org/10.4161/biom.28534

These drawbacks have been shown[7] to arise from the important residual internal stress induced in thermally sprayed coating during deposition. Indeed, a network of micro-crack developed in the ceramic coating volume in interface failures was induced.

Many Ca-P coatings on titanium have been done by immersing chemically-treated metal and polymer implants[8,9] in an aqueous solution containing calcium and phosphate ions at pH and physiological temperatures in order to simulate the biological process. Among chemical routes, the alkali–heat treatment of Ti followed by the biomimetic process seemed to be one of the most popular and effective methods.[10] Dipping in alkali solution produces a Na-containing titanate layer,[11] able to induce the deposition of Ca-P ceramics in vitro as well as in vivo. Other reports indicated that acid–alkali treatment on Ti implants[12-14] might be more effective for the deposition of a homogeneous bone-like apatite layer on the surface of Ti when immersed in simulated body fluid (SBF).[15] This biomimetic process imitates the growth of in situ-formed bone-like HA crystals.[16] Thus, the HA coating is more readily degraded by osteopath[17] overcoming many of the drawbacks associated with other deposition techniques, such as the processes utilizing high temperature treatment. It has also been proven that the chemical pre-treatment in alkali solution can improve the bonding between titanium substrate and calcium phosphate coatings fabricated by the subsequent biomimetic deposition in SBF.[18,19]

As an alternative technique for Ca-P coating, Oliviera, Leonor and Reis proposed to treat the surface of non-conducting materials such as polymers in an autocatalytic bath.[20-22] This method is based on redox reactions with electroless plating using palladium chloride ($PdCl_2$) as a catalyst. In this process, the $PdCl_2$ works as an arm of ionic change between the substrate and the solution.[20]

In the present study, we slightly modify this method and extend it to the growth of Ca-P layer on the metal substrate. After a mechanical polishing and a chemical treatment (e.g., using Kroll reagent) on the titanium substrate, a ceramic interlayer (sodium titanate, HT) is chemically generated by the action of an alkaline bath (NaOH), covalently linked to the metal substrate and ceramic coating. The alkaline pre-treatment on the Ti substrate and the further thermal treatments are performed in order to obtain a micrometric network layer (HT). Indeed, the Ca-P layer is produced using palladium chloride ($PdCl_2$, ACM1) or silver chloride (AgCl, ACM2) to activate the surface, according to Reis's method. This new deposition route has several advantages over plasma spray, pulsed laser deposition, as well as magnetron sputtering offering: an easy way to control the experimental conditions, the applicability to complex shapes, and especially no adverse effect of heating. Furthermore, this method is cost effective.

Results and Discussion

After the alkaline-heat treatment, a layer of titanium oxide (TiO_2) and sodium titanate ($Na_2Ti_nO_{2n+1}$, n = 3, 5, 6) was created on the surface of the metal according to previous works.[23,24] The structure of sodium titanate can be schematized in **Scheme 1**.

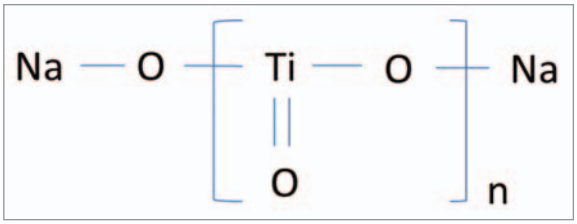

Scheme 1. Structure of $Na_2Ti_nO_{2n+1}$.

Table 1. Experimental lattice distances measured on SAED (**Figs. 1A and 2A**) recorded on ACM1 and ACM2 samples

ACM1 d_{exp} (± 0.005 nm)	ACM2 d_{exp} (± 0.005 nm)	Hydroxyapatite, ($Ca_5(PO_4)_3(OH)$, ICDD 09–432), d_{theo} (nm)	Calcium hydrogen phosphate hydrate, ($Ca_4H[PO_4]_3{\cdot}3H_2O$, ICDD 11–184) d_{theo}(nm)
	0.370		0.374
0.350	0.352		0.348
0.342		0.344	0.343
0.336			0.338
0.310	0.311	0.308/0.317	0.305
0.278	0.275	0.281/0.279/0.272	0.283/0.277/0.275
	0.207	0.207	0.208
0.194	0.197	0.194	0.195
	0.189	0.188	0.186
0.182		0.184	
0.175		0.175	

The Ca-P layer was then deposited by dipping the substrates into the baths ACM1 and ACM2. Their compositions are given in the experimental part. The layers were analyzed by XRD and the morphologies were observed by TEM and SEM techniques. No difference between both XRD patterns was observed; the patterns exhibit only the diffraction peaks of α-Ti and β-Ti structures showing that the sodium titanate and Ca-P layers are either too thin or made of so small crystallites that the peaks are too broad. The surface morphologies were examined by SEM (**Figs. 1C and 2C**). A dense coating made of nanoparticles is clearly observed on ACM1 (**Fig. 21**). The analysis shows that the layer is composed mainly of Ca and P. No sodium titanate network is detected. On the contrary, the ACM2 coating is less dense than the previous one as proved by EDS-X analyses. Indeed, Ca and P are detected as well as Na and Ti.

Typical TEM examinations of the scratched coatings are presented in **Figures 1A and 2A** for ACM1 and ACM2, respectively. The ACM1 collected particles appear to be in shape of rods of about 100–200 nm long while the ACM2 ones present more isotropic shapes in the 200–300 nm size range. Selected area electron diffraction (SAED) patterns, recorded on each sample (inserts in **Figs. 1A and 2A**), are characteristic for polycrystalline samples. The experimental lattice distances are given in **Table 1** and interpreted in terms of a mixture of hydroxyapatite ($Ca_5[PO_4]_3[OH]$,

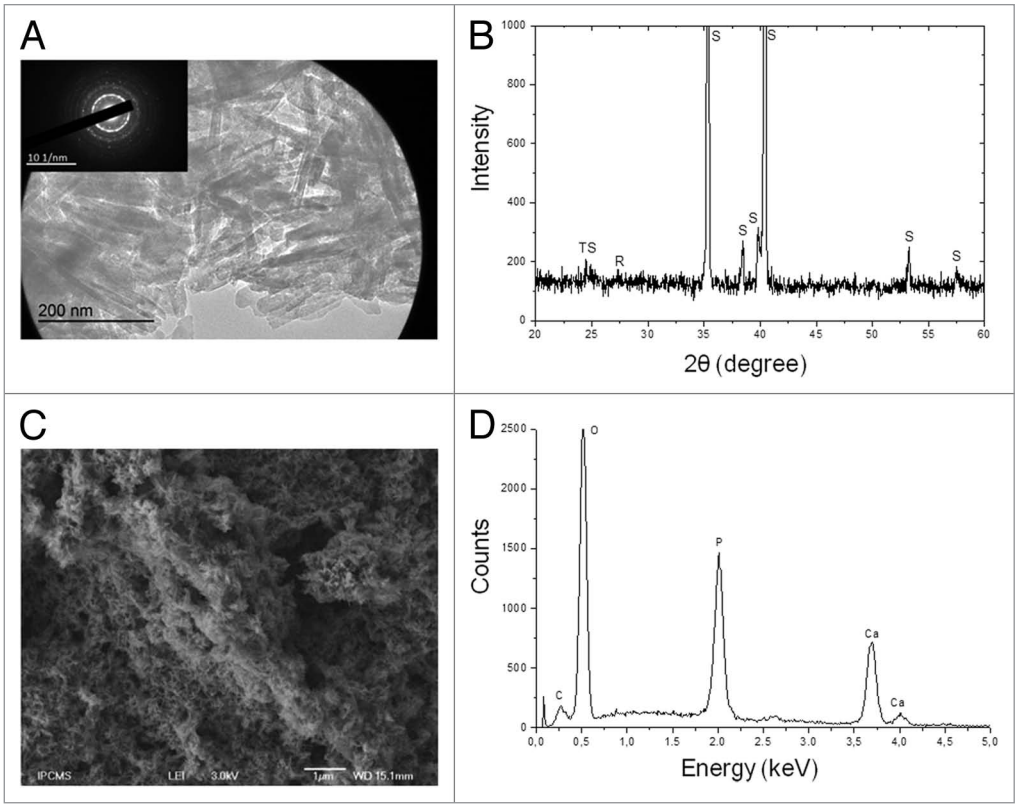

Figure 1. ACM1: (**A**) TEM observations on the scratched coating and the corresponding SAED pattern (insert). (**B**) XRD pattern, where TS is sodium titanate, R rutile, and S substrate. (**C**) Morphology by SEM and (**D**) corresponding EDS-X analyses.

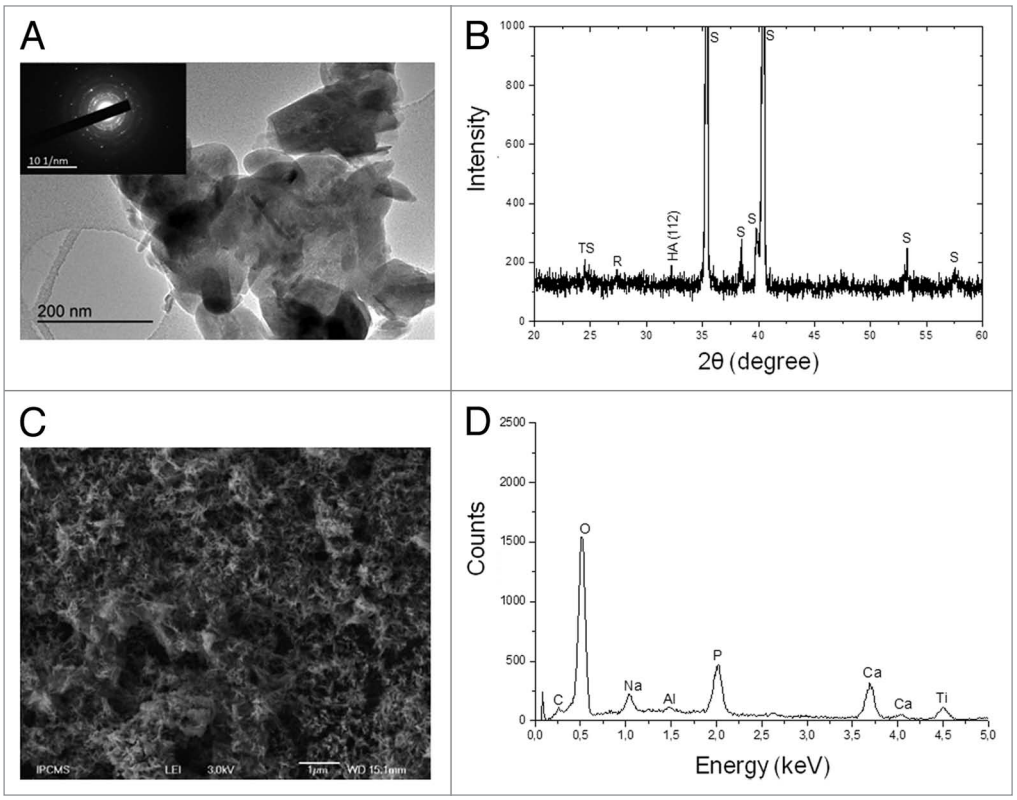

Figure 2. ACM2: (**A**) TEM observations on the scratched coating and the corresponding SAED pattern (insert). (**B**) XRD pattern. (**C**) Morphology by SEM and (**D**) the corresponding EDS-X analyses.

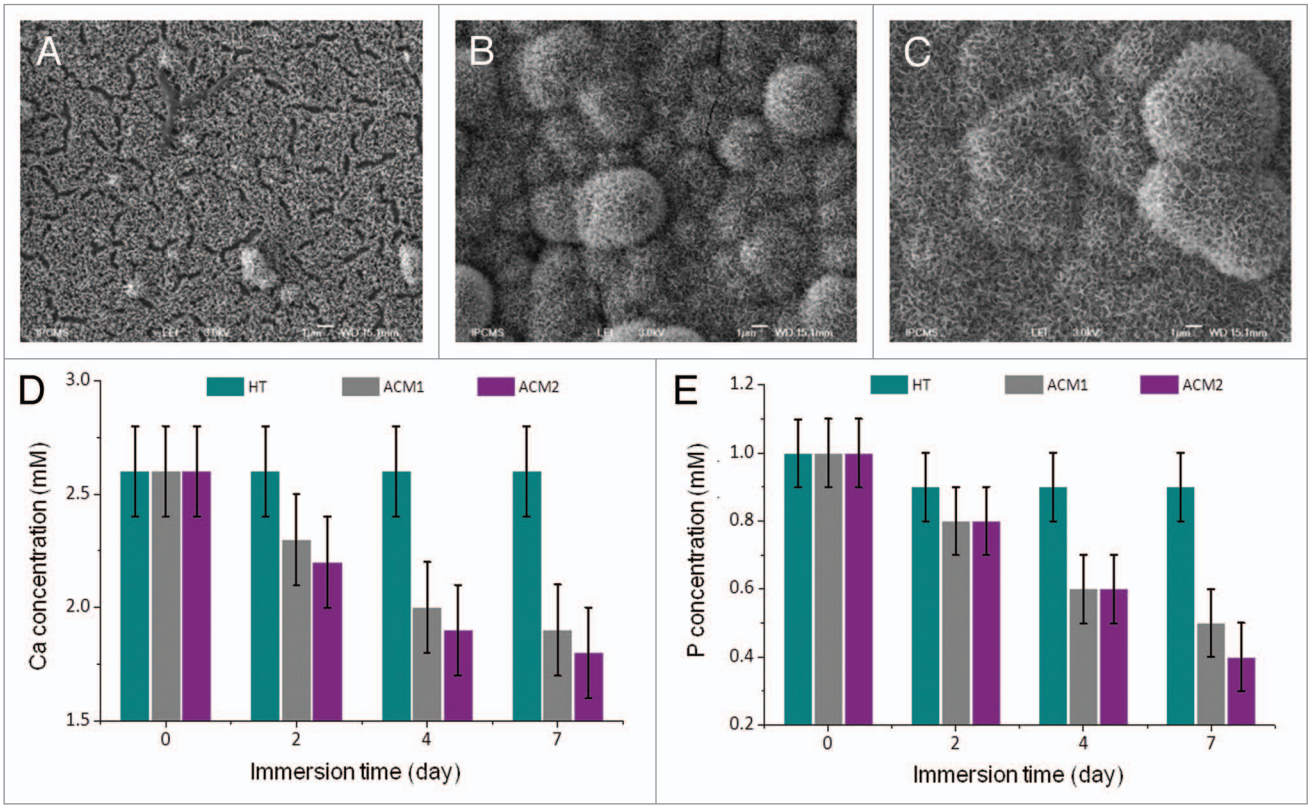

Figure 3. Morphology by SEM after one week in SBF (**A**) alkaline-heat treated titanium alloy (HT), HT treated after (**B**) ACM1 and (**C**) ACM2 baths. Concentrations of (**D**) Ca and (**E**) P ions in SBF1 after for 2, 4 and 7 d of the samples HT, ACM1 and ACM2.

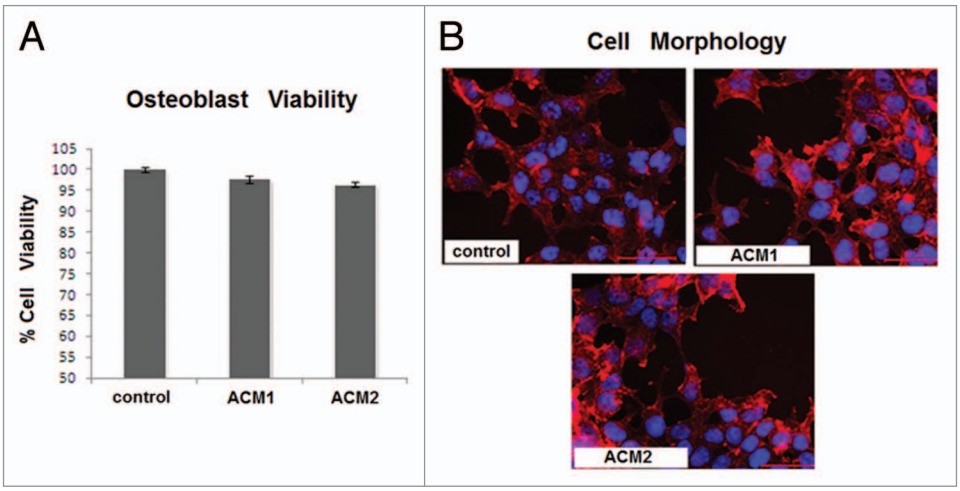

Figure 4. Direct cytocompatibility assay. Osteoblasts cultivated directly onto specimens' surfaces; the viability values are comparable to the control ones (**A**) and no statistical differences were calculated ($P > 0.05$). Bars represent mean and standard deviations. Moreover, the test and control cell morphology (phalloidin in red and DAPI in blue) is comparable as shown in (**B**). Bar scale = 50 μm.

ICDD 9–432) and calcium phosphate hydrate (calcium hydrogen phosphate hydrate, $Ca_4H[PO_4]_3 \cdot 3H_2O$, ICDD 11–184) on both ACM1 and ACM2.

Figure 3 shows the morphology of HT (**Fig. 3A**), ACM1 (**Fig. 3B**) and ACM2 (**Fig. 3C**) samples after immersion in SBF for 7 d. Ca and P concentrations after immersing the samples in SBF1 for 2, 4 and 7 d are given in **Figure 3D and E**. It was assumed that any change by decrease/increase in Ca or P concentrations, compared with the SBF reference solution, would represent a deposition/release on/from the sample surfaces respectively.

Ca or P ions release from SBF is observed after 2, 4 and 7 d for ACM1 and ACM2, (**Fig. 3D and E**). A sharp decrease in the ionic concentration of both Ca and P ions is recorded giving as result a dense Ca-P layer during all soaking periods (**Fig. 3B and C**).

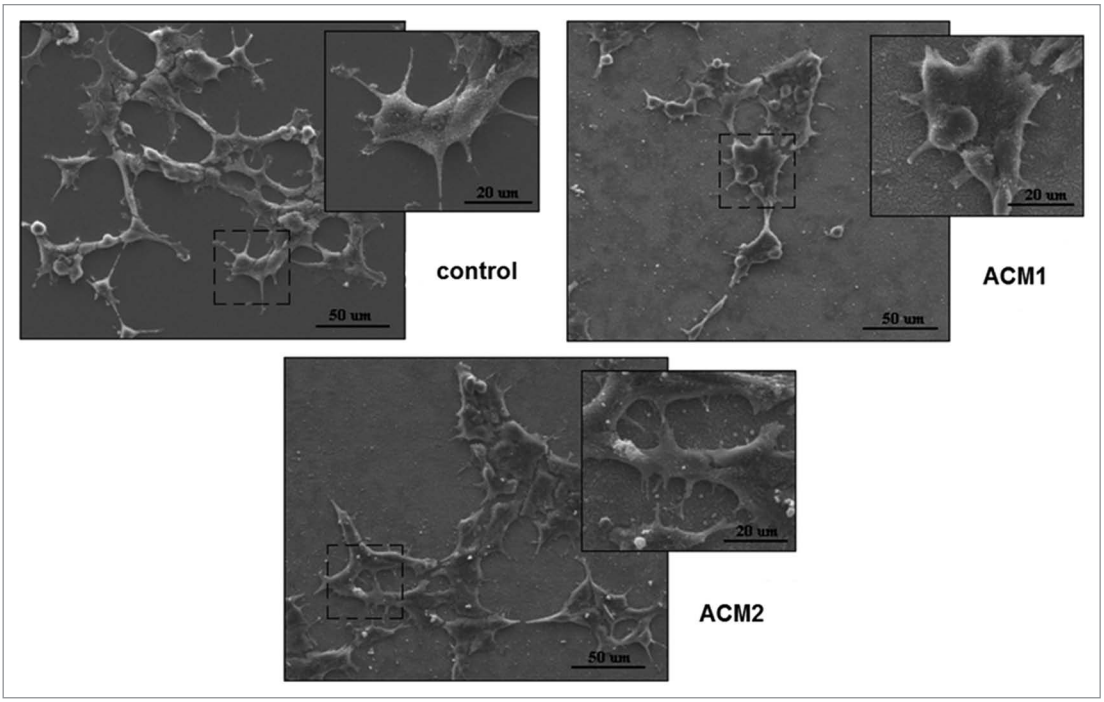

Figure 5. SEM images of osteoblasts seeded directly onto specimen surfaces after 24 h Control (upper panel, left) and treated (ACM1and ACM2) samples. The control samples morphology can be stated to be comparable.

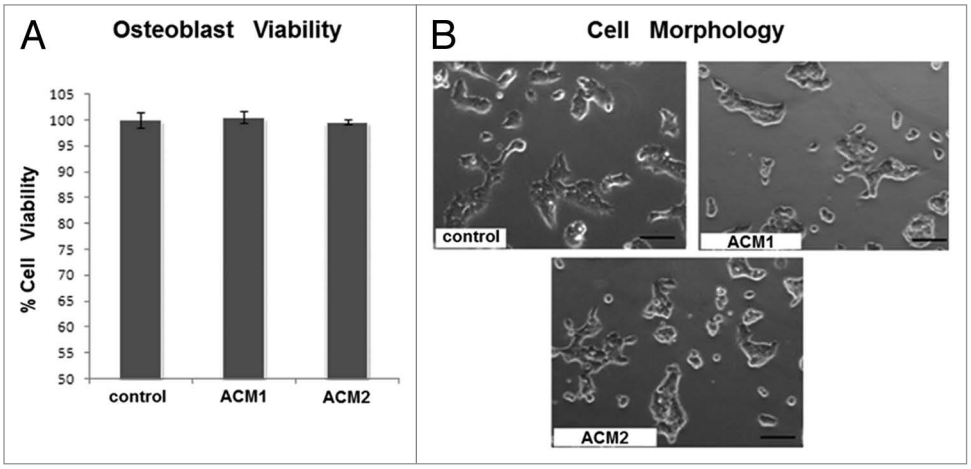

Figure 6. Non-direct cytocompatibility assay. Osteoblasts cultivated with medium stored one week in direct contact with treated samples; viability values are comparable with controls (**A**) and no statistical differences were noticed ($P > 0.05$). Bars represent means and standard deviations. Moreover, cells morphology and density investigated by light microscopy were comparable between test and control samples as shown in (**B**). Bar scale = 50 μm.

Differently, Ca ions for HT sample (**Fig. 3A**) are not modified, while P ions are slightly absorbed onto the surface.

Both tested specimens (ACM1 and ACM2) were not toxic for human osteoblasts. In fact, as reported in **Figure 4A**, the cell viability did not differ ($P > 0.05$) between control and test groups. Viability was observed onto experimental materials always higher than 95% with respect to control.

The viability assay results were confirmed by the morphological analysis; in fact, by immunofluorescence staining it is possible to appreciate the correct spread and density of cells cultivated onto experimental specimens surface that are comparable with the control (**Fig. 4B**). Also, SEM images confirmed the absence of morphological differences between cells cultivated onto treated samples and those onto the control material (**Fig. 5**).

Cells cultivated with the medium previously kept in direct contact for one week with treated samples showed a viability comparable with cells cultivated with the virgin medium (**Fig. 6A**). In fact, no statistical significant differences were observed between control and test samples. The cell viability was always registered higher than 98% of the control.

Visual investigation using light microscopy confirmed the viability assay results. As shown in **Figure 6B**, the cell morphology

and density are similar between control and test samples, suggesting that no toxic compounds were released into the medium by the treated specimens during the previous seven days of immersion.

These analyses show that Ca-P nanostructured layers made of hydroxyapatite $Ca_5(PO_4)_3(OH)$ and calcium phosphate hydrate ($Ca_4H[PO_4]_3{\cdot}3H_2O$) cover the titanium substrate well. The layer is thicker and denser when Pd is involved. The hypothesis made previously by Reis et al.[22] to explain the mechanism leading to the Ca-P deposition on polymers is schematized in **Figure** 7. First, palladium ions link onto the surface through the hydroxyde groups (**Fig.** 7**A**, step 1). Then, the negatively charged phosphate ions and the positively charged Ca ions are successively attracted so that this stacking results in the formation of calcium phosphate compounds (**Fig.** 7**B**, step 2). When silver is involved, a similar mechanism can be proposed. However, according to Reis et al., Pd ions are not eliminated. In case of Ag, the bath has the advantage to introduce ions known to have efficient antimicrobial properties[25]; moreover, as recently demonstrated by Alan BG Lansdown,[26] the pharmaceutical and toxicological profile of Ag in biomaterials shows that health risks associated with systemic absorption of silver as Ag are low.

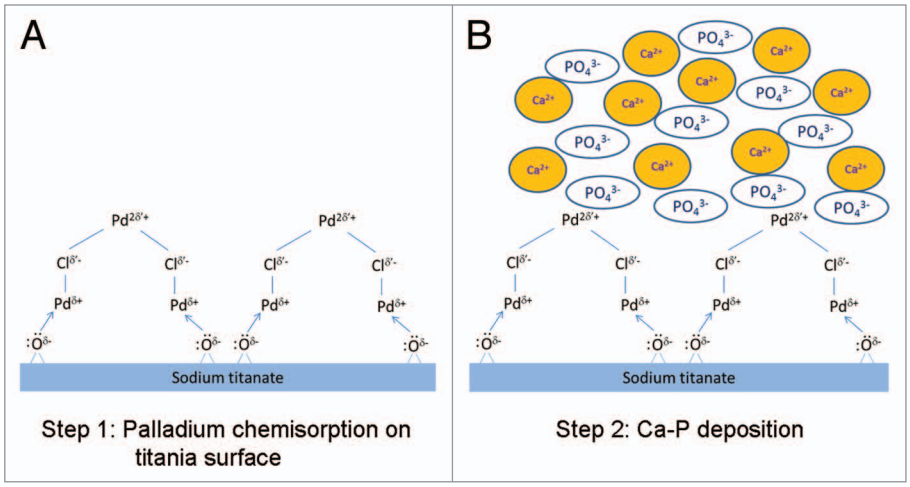

Figure 7. Hypothesis mechanism of Ca-P bioactive coating in the "activating" baths by using $PdCl_2$ as the catalyst.[22]

To create an osteoconductive titanium alloy, a new process route was applied. It consists of an immersion of Ti-6Al-4V in alkaline solution and a further heat treatment, followed by the immersion in a $PdCl_2$ or AgCl -containing baths. The obtained surface morphologies were optimized by the growth of porous sodium titanate layer. It was observed that the formation of HA and calcium phosphate hydrate was induced after 3 h immersion in ACM1 and ACM2 baths. The structure and morphology of the so-formed layers were characterized using several techniques.

These experimental treatments allowed producing cytocompatible materials potentially applicable to manufacture implantable devices for orthopedic and oral surgeries.

Materials and Methods

The samples were cut from a bar of commercially available Ti-6Al-4V ELI titanium alloy (chemical composition in wt.%: C, 0.013; Fe, 0.16; N, 0.014; H_2, 0.006; O, 0.11; Al, 6.05; V, 4.0; Ti, bal.). The specimens of 20 mm diameter and 1.5 mm thickness were abraded with SiC abrasive papers 240, 400, 1000, 2500, 4000 and polished to mirror with non-crystallizing colloidal silica suspension; then cleaned by successive ultrasonic treatments in acetone, ethanol and distilled water for 30 min. After mechanical polishing, the substrates were etched for 10 min in Kroll solution's reagent, a mixture of 0.045 M HF and 0.058 M HNO_3, at room temperature. The specimens were rinsed with distilled water and dried at 40 °C in an electric oven.

To form the sodium titanate hydrogel layer on the Ti-6Al-4V surface, the samples were dipped into a NaOH 10 M solution at 60 °C for 24 h and then thermally treated at 630 °C for 1 h with a heating rate of 5 °C/min.

To produce Ca-P coatings, the pre-treated specimens were soaked in two baths containing calcium chloride ($CaCl_2$) and phosphoric acid (H_3PO_4) and either palladium chloride ($PdCl_2$, ACM1) or silver chloride (AgCl, ACM2) under magnetic stirring for 3 h at (80 ± 2) °C and pH 5.3 ± 0.1. $CaCl_2$ acted as the source of calcium, while H_3PO_4served as a source of phosphate. The molar Ca/P ratio was 1.67. Then, the samples were cleaned in distilled water and dried in environmental conditions.

To evaluate the in vitro formation of Ca-P, the samples were soaked in simulated body fluid (SBF) solution at pH 7.4 using a buffer solution consisting of Tris hydroxymethylaminomethane and HCl, at body temperature (37 °C).[27] Ion concentrations of SBF solution and human blood plasma are shown in **Table 2**.

The change in Ca and P concentrations after 2, 4, 7 d soaking periods of samples was analyzed using the UV-Visible spectroscopy and Lambda 950 UV/VIS spectrometer (Perkin Elmer). After soaking, the specimens were washed with distilled water and dried at room temperature.

The Ca-P coatings were analyzed by X-ray diffraction (XRD) using a Bruker D5000 diffractometer equipped with a quartz monochromator and Cu Kα radiation (λ = 0.15406 nm). Diffraction scans were recorded in the 20–60° angular range with a 0.03° 2θ-step and a counting time of 4 s.

Scanning electron microscopy (SEM) observations of the coating morphologies were performed using a JEOL6700F equipped with an Energy Dispersive X-ray spectrometer (EDS-X). Images were recorded at 3 kV and EDS-X analysis at 10 kV on 10 × 10 mm^2 area and repeated three times at least.

The coated layers of samples ACM1 and ACM2 were scratched and collected on a microscope copper grid. Transmission electron

Table 2. Ion concentrations of SBF

	Concentrations of ions, mM								
	Na^+	K^+	Mg^{2+}	Ca^{2+}	Cl^-	HCO_3^-	HPO_4^{2-}	SO_4^{2-}	pH
Plasma body human	142.0	5.0	1.5	2.5	103.0	27.0	1.0	0.5	7.2- 7.4
SBF (type c)	142.0	5.0	1.5	2.5	147.8	4.2	1.0	0.5	7.4

microscope images (TEM) were recorded using a TOPCON 002B transmission electron microscope operating at 200 kV and equipped with a CCD camera and an EDS-X to analyze the chemical composition.

Human osteosarcoma cells (MG63, ATCC: CRL-1427) were cultivated at 37 °C, 5% CO_2 in Dulbecco's modification Minimal Essential Medium (DMEM, Sigma-Aldrich) supplemented with 10% fetal bovine serum (FBS, Lonza) and 1% penicillin-streptomycin. When the cells reached 85–90% confluence, they were detached by trypsin/EDTA (EDTA, Sigma-Aldrich), harvested and used for experiments.

Round specimens (15 mm diameter) were placed into 12 multi well plates (CellStar, PBI International); 2×10^4 cells/sample were seeded directly onto the surfaces of each specimen in a low volume of medium (200 μl) and allowed to adhere for 4 h prior to adding 2 ml of fresh medium to each well; plates were then incubated for 24 h at 37 °C, 5% CO_2. Afterwards, the cell viability was evaluated with the (3-[4,5-Dimethylthiazol-2-yl]-2,5-diphenyltetrazolium bromide) colorimetric assay (MTT, Sigma-Aldrich). Briefly, 100 μl of MTT solution (3 mg/ml in phosphate buffered saline [PBS]) were added to each sample and incubated 4 h in the dark at 37 °C; afterwards, formazan crystals were solved with 100 μl of dimethyl sulphoxyde (DMSO, Sigma) and 50 μl were collected and centrifuged to remove eventually debris. Surnatants optical density (o.d.) was evaluated at 570 nm with a spectrophotometer (Spectra Count, Packard Bell). Uncoated titanium o.d. was used as a control and considered as 100% cell viability while coated samples (named ACM1 and ACM2) viability was calculated as follows: (sample o.d. / titanium control o.d.) × 100. Experiments were performed 6 times for controls and each different coating.

Furthermore, the immunofluorescence staining was performed in order to investigate the cells morphology after 24 h of adhesion onto the biomaterials surface. Cells were fixed for 20 min with 4% paraformaldehyde at room temperature (RT) and then washed 3 times with PBS. Phalloidin (rhodamine B tetramethylisothiocynate, 1/2000 in PBS, AbCam) solution was added for 45 min (RT) in order to investigate cells cytoskeleton. Afterwards, the samples were washed 3 times with PBS and co-stained with 4',6-diamidino-2-phenylindole (DAPI, Sigma-Aldrich). The cells morphology was optically evaluated using a fluorescence microscope (Leica AF 6500, Leica Microsystems).

Serum free DMEM was incubated without cells for 1 wk at 37 °C, 5% CO_2 in direct contact with controls or coated samples in a ratio of 2 ml/specimens for a total of 10 ml/specimen. Afterwards, eluates were collected, supplemented with 10% FBS and used to cultivate MG63. Cells were seeded in a defined number (2×10^4 /well) into 24 wells plates (Cell Star, PBI International) and cultivated for 24 h at 37 °C, 5% CO_2. Afterwards, the cell viability was evaluated by the 3-(4,5 Dimethylthiazol-2-yl)-2,5-diphenyltetrazolium bromide colorimetric assay (MTT, Sigma) as described for the direct cytocompatibility assay.

SEM was used to investigate the morphology of cells seeded directly onto the specimens' surface. Briefly, after fixing, dehydration with the ascendant ethanol scale (70%, 80%, 90%, 100%), and hexamethyldisilazane, the specimens were mounted on aluminum stubs, using a conductive carbon tape, coated with a thin carbon layer (10 nm) and observed with a StereoScan 360 SEM (AbCam) at 10 kV with various magnifications, using secondary electrons.

Furthermore, the cells morphology was visually investigated after one week of cultivation by light microscopy (Leica AF 6500, Leica Microsystems).

Statistical analysis was done using Levene's test and ANOVA one-ways followed by Sheffè's post-hoc test using IBM® SPSS® Statistics 20 (IBM).

Disclosure of Potential Conflicts of Interest

No potential conflicts of interest were disclosed.

Acknowledgments

This work was supported by CAMPUS FRANCE-Centre français pour l'accueilet les échanges internationaux in the frame PHC IMHOTEP No. 25639NH and 20729TH. The authors take pleasure in acknowledging Guy Schmerber, Dris Ihiawa krim, Jacques Faerber for XRD, TEM, and SEM characterization respectively.

References

1. Liu X, Chu PK, Ding C. Mater Sci Eng Rep 2004; 47:49-121; http://dx.doi.org/10.1016/j.mser.2004.11.001
2. Brånemark P-I. Osseointegration and its experimental background. J Prosthet Dent 1983; 50:399-410; PMID:6352924; http://dx.doi.org/10.1016/S0022-3913(83)80101-2
3. Surowska B, Bienias J. J Achiev. Mater.Manuf. Eng 2010; 43:162-9
4. Dorozhkin SV. J Mater Sci 2007; 42:1061-95; http://dx.doi.org/10.1007/s10853-006-1467-8
5. Rosu RA, Serban VA, Bucur AL, Dragos U. Deposition of titanium nitride and hydroxyapatite-based biocompatible composite by reactive plasma spraying. Applied Surface Science 2012; 258:3871-6; http://dx.doi.org/10.1016/j.apsusc.2011.12.049
6. De Groot K, Geesink R, Klein CP, Serekian P. Plasma sprayed coatings of hydroxyapatite. J Biomed Mater Res 1987; 21:375-81; http://dx.doi.org/10.1002/jbm.820211203
7. Carradó A. Structural, microstructural, and residual stress investigations of plasma-sprayed hydroxyapatite on Ti-6Al-4 V. ACS Appl Mater Interfaces 2010; 2:561-5; PMID:20356205; http://dx.doi.org/10.1021/am900763j
8. Kokubo T. Apatite formation on surfaces of ceramics, metals and polymers in body environment. Acta Mater 1998; 46:2519-27; http://dx.doi.org/10.1016/S1359-6454(98)80036-0
9. Barrére F, Layrolle P, van Blitterswijk CA, de Groot K. Biomimetic calcium phosphate coatings on Ti6AI4V: a crystal growth study of octacalcium phosphate and inhibition by Mg^{2+} and HCO^{3-}. Bone 1999; 25(Suppl):107S-11S; PMID:10458288; http://dx.doi.org/10.1016/S8756-3282(99)00145-3
10. Wen HB, de Wijn JR, Cui FZ, de Groot K. Preparation of bioactive Ti6Al4V surfaces by a simple method. Biomaterials 1998; 19:215-21; PMID:9678870; http://dx.doi.org/10.1016/S0142-9612(97)00232-9

11. Kim HM, Miyaji F, Kokubo T, Nakamura T. Preparation of bioactive Ti and its alloys via simple chemical surface treatment. J Biomed Mater Res 1996; 32:409-17; PMID:8897146; http://dx.doi.org/10.1002/(SICI)1097-4636(199611)32:3<409::AID-JBM14>3.0.CO;2-B
12. Takeuchi M, Abe Y, Yoshida Y, Nakayama Y, Okazaki M, Akagawa Y. Acid pretreatment of titanium implants. Biomaterials 2003; 24:1821-7; PMID:12593964; http://dx.doi.org/10.1016/S0142-9612(02)00576-8
13. Kim HM, Miyaji F, Kokubo T, Nakamura T. Effect of heat treatment on apatite-forming ability of Ti metal induced by alkali treatment. J Mater Sci Mater Med 1997; 8:341-7; PMID:15348733; http://dx.doi.org/10.1023/A:1018524731409
14. Nishiguchi S, Kato H, Fujita H, Oka M, Kim H-M, Kokubo T, Nakamura T. Titanium metals form direct bonding to bone after alkali and heat treatments. Biomaterials 2001; 22:2525-33; PMID:11516085; http://dx.doi.org/10.1016/S0142-9612(00)00443-9
15. Kokubo T, Miyaji F, Kim HM, Nakamura T. Spontaneous Formation of Bonelike Apatite Layer on Chemically Treated Titanium Metals. J Am Ceram Soc 1996; 79:1127-9; http://dx.doi.org/10.1111/j.1151-2916.1996.tb08561.x
16. Kokubo T. Formation of biologically active bone-like apatite on metals and polymers by a biomimetic process. Thermochim Acta 1996; 280-281:479-90; http://dx.doi.org/10.1016/0040-6031(95)02784-X
17. Liu Y, Hunziker EB, Randall NX, de Groot K, Layrolle P. Proteins incorporated into biomimetically prepared calcium phosphate coatings modulate their mechanical strength and dissolution rate. Biomaterials 2003; 24:65-70; PMID:12417179; http://dx.doi.org/10.1016/S0142-9612(02)00252-1
18. Wang CX, Zhou X, Wang M. Mechanism of apatite formation on pure titanium treated with alkaline solution. Biomed Mater Eng 2004; 14:5-11; PMID:14757948
19. Tanahashi M, Matsuda T. Surface functional group dependence on apatite formation on self-assembled monolayers in a simulated body fluid. J Biomed Mater Res 1997; 34:305-15; PMID:9086400; http://dx.doi.org/10.1002/(SICI)1097-4636(19970305)34:3<305::AID-JBM5>3.0.CO;2-O
20. Leonor IB, Reis RL. An innovative auto-catalytic deposition route to produce calcium-phosphate coatings on polymeric biomaterials. J Mater Sci Mater Med 2003; 14:435-41; PMID:15348447; http://dx.doi.org/10.1023/A:1023214918592
21. Oliveira JM, Leonor IB, Reis RL. Carboxymethylchitosan/calcium phosphate, hybrid materials prepared by an innovative "auto-catalytic" co-precipitation method. Key Eng Mater 2005; 284:203-6; http://dx.doi.org/10.4028/www.scientific.net/KEM.284-286.203
22. Oliveira JM, Costa SA, Leonor IB, Malafaya PB, Mano JF, Reis RL. Novel hydroxyapatite/carboxymethylchitosan composite scaffolds prepared through an innovative "autocatalytic" electroless coprecipitation route. J Biomed Mater Res A 2009; 88:470-80; PMID:18306322; http://dx.doi.org/10.1002/jbm.a.31817
23. Yamaguchi S, Takadama H, Matsushita T, Nakamura T, Kokubo T. J Ceram Soc Jpn 2009; 117:1126-30; http://dx.doi.org/10.2109/jcersj2.117.1126
24. Wei M, Kim HM, Kokubo T, Evans JH. Mater Sci Eng C 2002; 20:125-34; http://dx.doi.org/10.1016/S0928-4931(02)00022-X
25. Chaloupka K, Malam Y, Seifalian AM. Nanosilver as a new generation of nanoproduct in biomedical applications. Trends Biotechnol 2010; 28:580-8; PMID:20724010; http://dx.doi.org/10.1016/j.tibtech.2010.07.006
26. Lansdown AB. A pharmacological and toxicological profile of silver as an antimicrobial agent in medical devices. Adv Pharmacol Sci 2010; 2010:910686; PMID:21188244; http://dx.doi.org/10.1155/2010/910686
27. Kokubo T, Takadama H. How useful is SBF in predicting in vivo bone bioactivity? Biomaterials 2006; 27:2907-15; PMID:16448693; http://dx.doi.org/10.1016/j.biomaterials.2006.01.017